CHAPTER 2

Literature Review

2.1 Dye-sensitized solar cell

The dye-sensitized solar cell (DSSC) has been developed over a few decades. The DSSC takes a role as a low cost solar cell with fine power conversion efficiency approximately 11.0 % [1] compared with other types of solar cell which have their highest converting efficiency as 44 %, their cost is high when compared to DSSC. Its efficiency depends on several causes: porosity of the oxide electrode, molecular dye that absorbs sunlight and its electrolyte solution.

In the present time, the oxide electrode has discovered that the porous titanium dioxide nanoparticles provide higher power conversion compared to other oxide compound, e.g. Zinc oxide [8].

The dyes are effective for absorbing photon and converting them to energetic electrons. Most of the energy loss due to the conduction in the TiO_2 layer. The efficiency varied by the varying of solar cell design.

2.2 Titanium dioxide

In the atmospheric condition, the titanium dioxide (TiO_2) can be found in several main phases: rutile, anatase and brookite as shown in Figure 2.1, where white and red spheres represent titanium atoms and oxygen atoms respectively. Rutile structure is the most abundant approximately 98% found in the atmospheric pressure [9], while anatase and bookite can be converted to rutile upon heating. However, the anatase contains both photovoltaic and photocatalytic properties of TiO_2 which is preferred for the study [10].

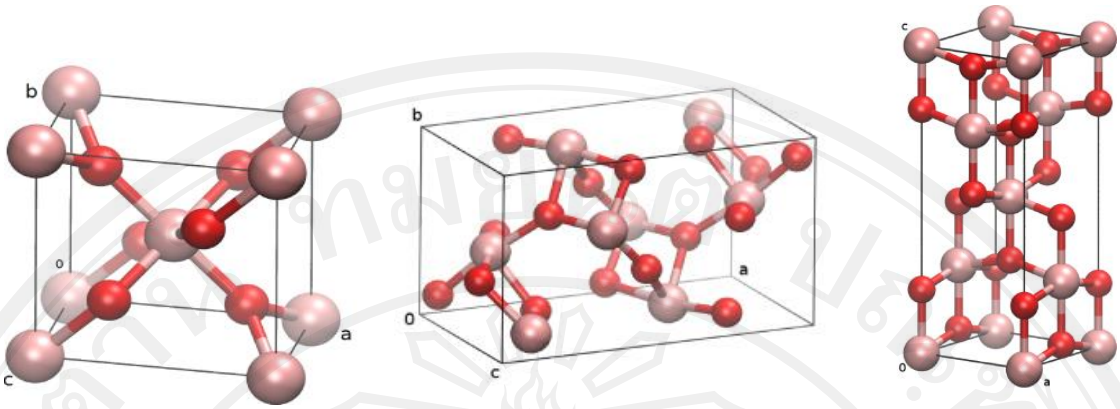

(a) (b) (c)

Figure 2.1 Unit cells of 3 main phases of TiO_2; (a) rutile, (b) brookite and (c) anatase structure.

Because of each phases consisted of different structure of Ti-O bonding which causes in their differences in properties, as a result their band gap energy are different, which causes the differences in photovoltaic and photocatalytic activities. Moreover the rutile, brookite and anatase have their band gap energies at 3.02 eV, 3.14 eV and 3.20 eV respectively, which are UV active. Therefore, the main three phases are able to show their photovoltaic and photocatalytic activities under the absorbing UV radiated from the sun.

The brookite phase is not widely studied due to its nature. The phase usually found as a mixed structure with anatase. Therefore the brookite phase will not be mentioned so often in this study compared to the other two phase [11]. The comparison of the photovoltaic and photocatalytic properties of rutile and anatase are widely studied. There are several reasons which support that the anatase phase's properties are better than the rutile's[12].

To begin with the relative position of the conduction band minimum (CBM) in rutile and anatase are different. The anatase has a larger band gap than the rutile suggest the CBM in anatase to be higher than in the rutile, as a result the conduction band of anatase is lower than the rutile.

Anatase has its indirect band gap that is smaller than its direct band gap. While the rutile has very similar between the direct and indirect band gap. Normally, semiconductors with indirect band gap which is similar to its direct band gap provides

longer charge carrier life times compared to direct gap materials. A longer life of electron-hole pair in anatase compared to rutile causes the charge carrier to participate in reactions.

2.3 Diamond-Like Carbon

Carbon is a very versatile element that crystallizes into diamond and graphite structures. In general, an amorphous carbon film can have any mixture of sp^3, sp^2, and even sp^1 sites, with the possible presence of hydrogen and nitrogen. An amorphous carbon with a high fraction of diamond-like (sp^3) bonds is known as diamond-like carbon (DLC) especially the tetrahedral amorphous carbon (ta-C) which is informed its compositions in Table 2.1 and its structure in Figure 2.2 and Figure 2.3. Unlike diamond, DLC can be deposited at room temperature, which is an important practical advantage. DLCs possess a unique set of properties, which has led to a large number of applications such as magnetic hard disk coatings; wear-protective and antireflective coatings for tribological tools, engine parts, razor blades, and sunglasses; biomedical coatings (such as hip implants or stents); and microelectro mechanical systems [13].

Table 2.1 Comparison of major properties of amorphous carbons with those of reference materials diamond, graphite, C_{60} and polyethylene

Amorphous carbons	sp^3 (%)	H (%)	Density (g cm^{-3})	Gap (eV)	Hardness (GPa)
Diamond	100	0	3.515	55	100
Graphite	0	0	2.267	0	
C_{60}	0	0		1.6	
Glassy C	0	0	1.3-1.55	0.01	3
Evaporated C	0	0	1.9	0.4-0.7	3
Sputtered C	5	0	2.2	0.5	
ta-C	80-88	0	3.1	2.5	80
a-C:H hard	40	30-40	1.6-2.2	1.1-1.7	10-20
a-C:H soft	60	40-50	1.2-1.6	1.7-4	<10
ta-C:H	70	30	2.4	2.0-2.5	50
Polyethylene	100	67	0.97	6	0.01

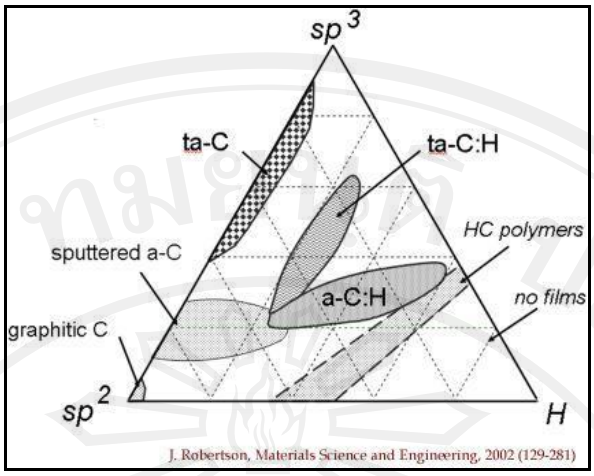

Figure 2.2 The various phases of diamond-like carbon [1].

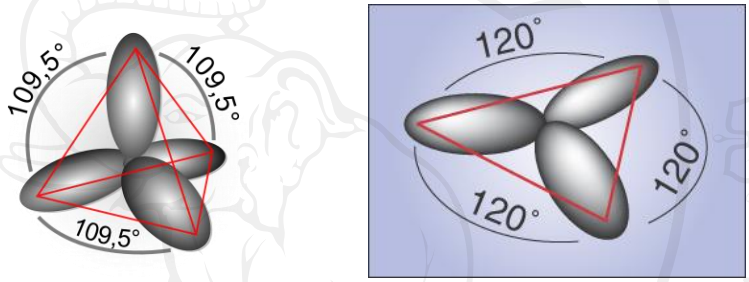

(a) (b)

Figure 2.3 Components of a DLC material; (a) sp^3 hybridization, (b) sp^2 hybridization.

In recent years, DLC has been applied as a protection layer of Hard disk drive as shown in Figure 1.4. The film is very thin on the order of 10-20 nm. The ideal material for this would be tetrahedral amorphous carbon (ta-C) because of its high density, high C-C sp^3 content, and unique surface properties. Especially the film properties are independent of the film thickness, thus providing films of equal qualities whether it is 1 nm or 100 nm thick. This material can be grown with deposition techniques involving energetic ions, such as filtered cathodic vacuum arc (FCVA). 'Vacuum arc' is a term used to describe a direct current (DC) glow discharge involving the explosive emission of plasma from the surface of a conductive electrode. The electrode material itself is used to sustain the discharge without the need for a background gas and the process can therefore occur under vacuum. When the plasma material is emitted from the cathode surface the term 'cathodic vacuum arc' is used. Emission from the anode surface is also possible under certain conditions, thus termed 'anodic vacuum arc'. The cathodic arc is mostly used in most application because of the efficiency in producting metal plasma

and its simplicity. These are basic features that make it well suited for film deposition application. Cathodic arc can operate in both pulsed and DC or continuous modes. The advantage of pulsed operation is mainly related to the significant reduction requirement of good cooling.

However, the DLC film characteristics and quality are found to be very much dependent on FCVA parameters and conditions. These include substrate materials, substrate surface preparation, total number of pulses, pulse frequency, target holder bias, chamber base pressure, background gas species, arc power supply parameters such as voltage and current, cathodic rod installation geometry, etc. All of these conditions must be complicatedly coordinated to achieve required DLC film qualities. Therefore, the present study represents the investigation of DLC film formation with FCVA by varying bias voltage of 0 V, -150 V, -250 V, -350 V and -450 V with N_2 partial doping pressure of 0, $9x10^{-5}$, $2x10^{-4}$, $5x10^{-4}$ and $3x10^{-3}$ torr with base pressure $5x10^{-5}$ torr deposited for 10 minutes with various Nitrogen partial pressure levels.

2.4 Filtered cathodic vacuum arc deposition

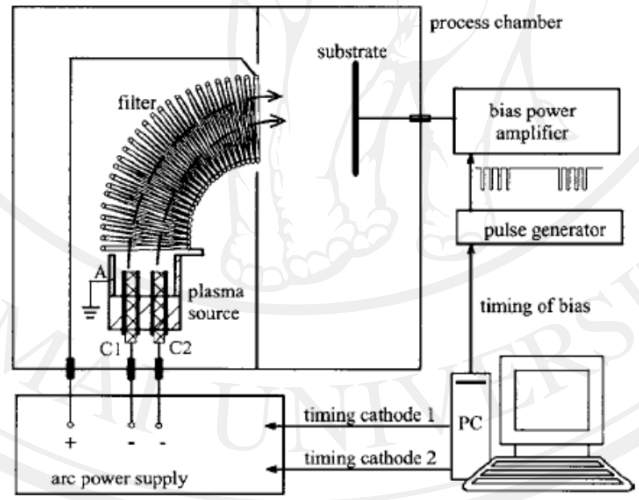

Figure 2.4 Schematic of FCVAD system.

Filtered Cathodic Vacuum Arc Deposition (FCVAD) is an effective ion deposition technique shown in Figure 2.4, which is able to produce a very high ion deposition rate, high adhesion and very clean thin film. To begin with electrons and ions are produced at a “Cathode spot” on plasma source after applying a very high current (1-10A) with low voltage (a few hundred Volts) onto the source. “Vacuum Arc” represents the vacuum condition between the electrodes before the arc discharge is emitted. Moreover an

important part to reduce a large number of macroparticles to degrade a synthesized film is the macroparticle filtering. In additions, the filtered plasma beam deposits on a negative biased substrate.

There are three parts of FCVAD system, which work together. Cathodic arc source is a part where ions, electrons and macroparticles are produced. Magnetic filtering coil helps filtering macroparticles, which take a major cause to degrade the film quality. The substrate's biasing part, which applies a negative potential on a substrate. And the reactive gas flow system, which flow a reactive gas into the vacuum chamber in order to react with deposited ions.

2.4.1 Cathodic Arc Sources

Most of commercial cathodic arc deposition systems are operated in the continuous direct current mode, which are characterized by a high deposition rate and low cost. It can produce its arc current between 40 to 150 A. However, it is limited by the upper limit current due to its installed cooling system. In principle, the arc current can be much higher than 150 A, which causes higher plasma production and deposition rate, but increasing of heat problems of plasma source and substrate, increasing cost for power supply and the contaminating of macroparticles on a substrate [14].

Some applications can be achieve with higher quality of deposited material by applying pulsed arcs, which offers several advantages over continuous DC operation. The power consumption is easily regulated via the arc duty cycle rather than the arc current. Spot steering is not an issue since the arc spots travel only a short distance from the point of ignition. Ignition can be designed to occur in the center of a cathode with the arc spots repel to each other. By this approach, the pulse is conveniently chosen when the spots arrive at the cathode rim, ensuring rather uniform cathode erosion. Pulsed arcs can be operated with very high pulsed currents, and therefore the average plasma production may approach those of DC arcs. The comparison of the DC and pulsed arcing depositions has shown in Table 2.2.

Table 2.2 Two types of cathodic arc sources which named by its applying current; continuous direct current (DC) and pulsed current. [14]

	DC	Pulsed
Deposition rate	High	Typically only a few percent of DC, through can be scaled to DC values
Cost	Low	Wide range, from very low for small experimental system to moderate for high rate system
Macroparticle production and incorporation in film (assuming no filter)	Moderate to high when operation in the absence of reactive gas, cathodes of low melting temperature, and less than perfect cathode cooling	Less than DC under otherwise comparable conditions
Incorporation of hydrogen and other contamination	Very low	Can be high, especially for low duty cycle system and substrate near room temperature
Power consumption and cooling requirements	1 kW or greater per arc source, cooling must match this input power	Small for low duty system (may not even need water cooling) to high for system that match DC deposition rate (high current, high duty cycle)
Trigger requirement	Mechanical trigger is adequate	Electronic trigger system often involving higher voltage (>1 kV)
Scaling options	Can be scaled to elongated cathodes, or ganged for large area coatings	Typically used as point sources, may be ganged for large area coatings

Because of their simplicity in terms of applying power and cooling demands, the pulsed arcs are often applied in research and development system. In addition, the pulsed system can produce drastically lesser amount of neutrals than DC system, such as from evaporating macroparticles and cooling spot craters. Moreover, the pulsed system produces more states of ion charge and ion energy, which affect the film properties. In additions, coating produced by pulsed arcs tended to have greater incorporation of hydrogen and oxygen (which is preferred in this research) but the DC arcs produce very little hydrogen and oxygen composition content on films. The contamination can be raised their amount by applying shorter pulses, low duty cycle arcing and non-heated substrates.

It can be concluded that, the applying pulsed current system is using in this study due to its simplicity and low cost, avoid dealing with problems from heat, contaminating of oxide on films are required. Therefore, this research will focus on using a pulsed arc source for deposition.

In addition, Applying arc current and ion current is not exactly the same, the ion current is approximately 1-20% of the applying arc current, which depends on the different kinds of cathode as shown in Figure 2.5 below.

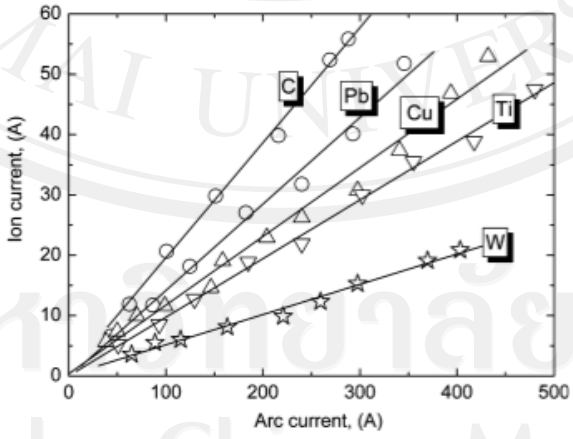

Figure 2.5 Ion current from different elements plotted as a function of arc current [14].

Increasing of the arc current causes more ion current. As a result, there are more particles emit from the cathode.

However, measuring an applying arc current directly is not easy due to varying overtime in a constant range, measuring of its arc voltage is a lot easier. Therefore, this study will obtain an arc current from converted arc voltage.

The pulsed arc sources can be separated into two types depend on applied curre7nt: Miniature sources and High-current Pulsed arc sources [14].

1) Miniature Sources

The miniature source is in uses for the study. It has a small "footprint" in several respects: size, cost, power consumption, cooling requirement, flexibility of mounting, variable duty cycle. However, the duty cycle is usually chosen to be small in order to avoid heating problems on temperature-sensitive materials (like plastics). In additions, the reason for using of miniature source is the working area of cathode can be made small. Thus, the location of plasma production can be well defined.

Miniaturized arc sources need to be worked with average applying power to the cooling capabilities [14]:

$$\bar{P} = \int \frac{I_{arc} V_{arc}}{(t_{on}+t_{off})} dt \qquad (1)$$

If the current is approximately constant during the pulse on-time, the integral can simply be approximated by $\int I_{arc} V_{arc} dt = I_{arc} V_{arc} t_{on}$. Thus, the (1) can be re-written as

$$\bar{P} = d I_{arc} V_{arc}$$

where d designates the duty cycle,

$$d = \frac{t_{on}}{\left(t_{on} + t_{off}\right)}$$

In case of absence of water cooling system, the duty cycle must be very small, typically $d < 1\%$. Therefore, the deposition rates from miniaturized sources are naturally much smaller than the rates obtained with DC arc sources. Due to the pulsed nature, miniature arc sources are commonly equipped with and electric trigger system. The size of miniature arc sources were designed to be small cathode rods whose diameter ranged from 3.12 mm to 12.5 mm as shown in Figure 2.6 [14].

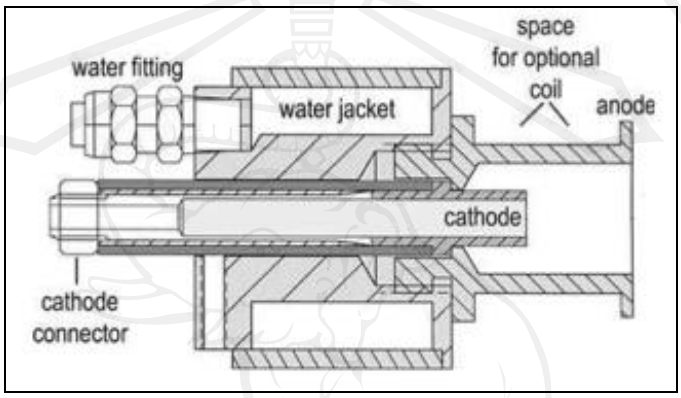

Figure 2.6 Schematic of a 1995 Berkeley Lab's miniature cathodic arc source, a popular low-cost system is suitable for research and developing applications.

2) High-Current Pulsed Arc Sources

As an equal applying current on a pulsed arc system and DC system, pulsed arc system cannot achieve higher deposition rate than the other. However, the pulsed arc system can offer a very high arc current pulsed (> 1 kA) at high pulse duty cycle. The plasma production is approximately proportional to the power of the arc discharge. Since the discharge voltage is constant when higher currents are used, it is common to refer to the arc current (not power) as the output scaling parameter.

2.4.2 Macroparticle Filters

Not only ions and electrons are produced at the source but macroparticles are also produced either. However, there is the most successful method to deal with macroparticles issue by utilizing curved macroparticle filters[14].

Filters are applied to separate and remove macroparticles from the produced cathodic arc plasma, which causes improving the quality of cathodic arc thin films coating. Without using of the filter, the coating films are rough and structurally and chemically not uniform.

The general idea of most macroparticle filters separate the macroparticle by electromagnetically guiding of plasma to substrate, which is placed out-of the line of sight with the cathode. For example, a bended solenoid helps filtering the macroparticles by providing a bended magnetic field. Because of large inertia and small charge, the trajectories of macroparticles are not affect by the field. As a result, the particles are lost in the filter. The straight filters are also used for other objectives.

Macroparticle filtering is usually done with curved magnetic filters (with 90 degree filter duct), the electron gyration radius is much smaller than the filter radius, while ion motion is only little affected by the magnetic field. In the conditions, the magnetic field lines are approximately equipotential lines forming an electric potential “valley”. The potential channel guides charged particles through the filter.

Various designs of filters have been described in the literature. It seems that the tighter filter curvature and longer filters would reduce the amount of macroparticles as well as greater loss of plasma. As a result, the ratio of plasma to macroparticles should be more considered, rather than the absolute reduction in macroparticle’s number density.

1) Filter efficiency

Not every filter-entering ions will coat on a substrate. Some of them may be lost to the filter wall by diffusion and other mechanisms and therefore it is important to consider parameters that characterize the performance of a filter. The plasma transport efficiency of a filter is considered as the number of filter-exiting particles per the filter-entering particles per time unit [14]:

$$k_{eff} = \frac{N_{i,exit}}{N_{i,enter}}$$

However, it is practically difficult to measure these quantities. Therefore, there are variables which offers more comfortable and useful, to define the filter efficiency.

2) System coefficient

The figure of merit has evolved into the system coefficient, can be defined as the ratio of filtered ion current to arc current[14]:

$$k = \frac{I_i}{I_{arc}}$$

These variables are easier to use, because the amount of plasma produced at cathode spots is proportional to the arc current. Literature reports that the system efficiency for filtered arcs about 0.5-1% [14].

For pulsed systems, it is not convenient to calculate the system efficiency from a non-constant current. However, the pulsed systems can define the system efficiency as

$$K = \frac{\int_0^{t_{pulse}} I_i(t)dt}{\int_0^{t_{pulse}} I_{arc}(t)dt}$$

where the integration is over the pulse duration t_{pulse}.

The system coefficient provides more convenient to compare the efficiency of different filters and source configuration.

However, comparison of the different cathodes' coefficient is not recommended, due to each cathode material has its characteristic ion erosion rate and ion charge state distribution. Although, the ion charge state distributions and their mean ion charge states are known. The ion erosion rates depend on cathode material, thermal, geometric and electrical specifics of the discharge system.

3) Motion of charged particles in Filter

The plasma stream contains electrons, ions, neutral atoms and macroparticles. The neutral atoms and macroparticles are not affected by bended magnetic field produced from a curved magnetic filter. Although, ions are more interesting in coating, without attraction from guiding electrons, the ions cannot coat on a substrate.

The motion of charged particles; electrons and ions, in electromagnetic fields can be simply described by the equation of motion

$$m\frac{d^2r}{dt^2} = Qe(\mathbf{E} + \mathbf{v} \times \mathbf{B}) \qquad (2)$$

where v is the velocity of the particle when it is emitted from the ion source, m is the particle's mass, Q is the charge number of the particle and e is the electron's charge constant. However, E and B are not only consisted of external fields but also affected by presence and motion of all charged particles. In fact, the equation is in a simple form. Several methods to improve the equation are required.

It is a simple method to calculate the particle's gyration radii by assume that the external electric field in the equation (2)

to be zero. For an electron which has its mass as 0.0005 u (unified atomic mass unit; 1 u = $1.660538921 \times 10^{-27}$ kg) where The induced magnetic field strength for filter is around 10-100 mT, therefore the gyration radii of an electron is around 3.5×10^{-5} m. Differently for the titanium ion (47.86 u), the ion gyrates as a very large radius (3.4 m) compared to the filter diameter (less than 5 cm). It can be concluded that the ion does not gyrate under the filtering process.

Moreover, the emitted electrons which move faster than titanium ions, also drags the ions to deposit on a substrate.

2.4.3 Substrate's biasing system

In case of floating wall (grounded substrate), the neutral wall will be firstly deposited with electrons which come from filtering coil, causes negative charge arranging on the wall's surface. Then the following ions will deposit on the wall. Similarly for negative biased wall, the ions will also deposit on the wall but they have more kinetic energy caused by negative potential biased wall.

More negative biasing voltage causes the deposited film becomes higher adhesion[14] and more dense. A very high voltage -1,000 V biasing causes ions implanting on the substrate. However, the expected specification of the film is the anatase titanium dioxide thin film need to have a high porosity, which costs its density and adhesion without implanting into a substrate surface.

2.4.4 Reactive gas flowing system

Many applications of cathodic arc appear as the compound of the cathode with reactive gas. Reactive gas takes a major role for utilizing depositing a film which contain an element comes from the gas. For example, titanium nitride cannot be able to directly deposit on a substrate without filling a deposit chamber with nitrogen gas. Similarly for depositing titanium dioxide film, doping of oxygen is required. After emitting of plasma, the emitted energetic electrons causes direct impact

ionization of the doping gas. While the gas is ionized, the emitted ions bond with the ionized gas and forming into a compound, which is consisted of the element of ion and gas. In despite of DLC, the reactive gas is not necessary because DLC is consisted of a pure carbon element; however, some kinds of reactive gas do help improving the DLC's adhesion.

2.4.5 Arc source integration in Coating Systems

The coating systems can be separated into 2 types sorted by the purpose of using the coated materials: Batch systems and In-Line systems[14].

The most of all cathodic arc system are defined as a Batch system. Because of the application need only a step of deposition. Such as coating of a drill to improve its toughness, the coating of a layer of diamond-like carbon is fine. In contrast, an In-line coater can provide a large production which is more preferred as an industrial scale of coating. Because the coating has more than a step of deposition process such as the coating of a computer harddisk, which needs to coat a harddisk with several times with different cathodes. By inputing a non-coating harddisk into its in-line coating machine, the whole processes take around a few hours to provide a coated one.

2.5 Annealing of the film

Annealing of the film with high annealing temperature utilizes changing of the film structure. Since the thin film is composed of crystalline and amorphous structures. Amorphous structure can be morphed into crystalline structure by annealing [15]. Moreover, the higher temperature annealing process also causes more roughness on the film [16].

However, annealing titanium dioxide thin film is not suitable for annealing at high temperature above 800^{o}C. Because, the anatase structure which takes a major role in photovoltaic and photocatalytic process, change into the most stable structure rutile and also decrease the film's porosity [17].

It can be concluded that the annealing of the film is necessary for forming the TiO_2 structure into the anatase. However, too high annealing temperature is not suggested.

2.6 Analysis technique

In this study, there are several analysis techniques required for investigating deposited TiO_2 film. Scanning Electron Microscopy is applying for investigating the surface of the film, Raman Spectroscopy for determining structures of the film whether the anatase structure is deposited, Atomic Force Microscopy with scanning mode stand for the film's morphology and thickness.

2.6.1 Scanning Electron Microscopy and Energy-Dispersive Spectroscopy

Scanning electron microscope provides two useful analysis techniques; Scanning Electron Microscopy technique (SEM) analyze and display a high magnification image of material up to 10,000,000x better than any optic microscopes do. Moreover the Energy-Dispersive X-ray Spectroscopy (EDS or EDX) also provide a both quantitative and quality analysis of the material. Although these two techniques are used for different purposes due to detecting of different phenomenon, the process of producing of an electron beam is the same.

1) Providing an incident electron beam

An electron gun (hot cathode source) made of heated tungsten filament produces an electrons cloud, which would be accelerated by electrodes as shown in Figure 2.7.

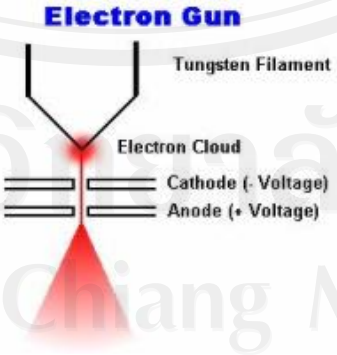

Figure 2.7 Schematic of a SEM's installed electron gun [18].

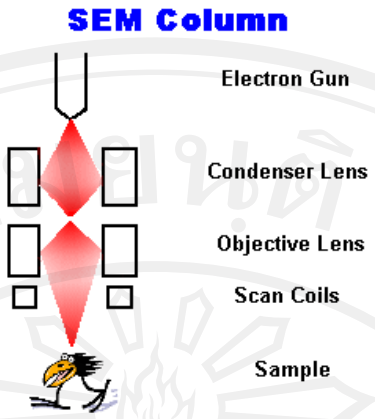

Figure 2.8 Schematic of an arranged SEM's instruments.

The accelerated electrons beam is focused by a set of electromagnetic lens onto a sample as shown in Figure 2.8. The electromagnetic lenses are consisted of a condenser lens, objective lens and scan coil. The condenser lens controls the sized of the beam, increasing of the size of the beam achieves a better signal with lower noise but reducing the resolution. Depending on the magnification, the relationship between signal to noise and resolution achieves the best image quality. The objective lens focuses the beam onto the sample, which is necessary to have a proper focus image. Moreover, the scan coils are placed around the beam in both x and y direction to provide a x-y direction beam scanning over the sample's surface.

2) Scanning Electron Microscopy

While bombarding an electron beam onto the sample, the bombarding electron beam incident onto the sample's inner shell electron which is knocked off from its orbit and called the secondary electron, and detected by a secondary electron detector. After detecting the electron, a digital signal is provided and displayed as a monochromatic formed image of sample's surface.

In order to increase the magnification of the surface image, reducing the size of the area by the scan coils is required.

3) Energy-Dispersive X-ray Spectroscopy

While bombarding an electron beam onto the sample, not only secondary electrons are emitted but the characteristic x-ray is also emitted too. The x-ray is emitted by the outer electrons which reduce their energy to fill the atom's vacant inner orbit whose electrons are just knocked by the electron beam. Therefore the composite elements in the sample can be identified by their characteristic x-ray as well as their quantity.

4) Method of using EDS

After electron bombarding on the substrate and knocking of the inner shell electrons, the outer shell electron: e.g., L and M-shell, emit its energy to reduce its orbital shell into the vacant ground state shell K-shell, the transition processes are called K_a and K_b respectively as shown in Figure 2.9. The energy emitted as the characteristic x-ray which is different for each element. Both of the characteristic X-rays' energy and amount are both detected by an energy-dispersive spectrometer. Therefore the information obtained from the technique is the sample's composition's quantity and quality.

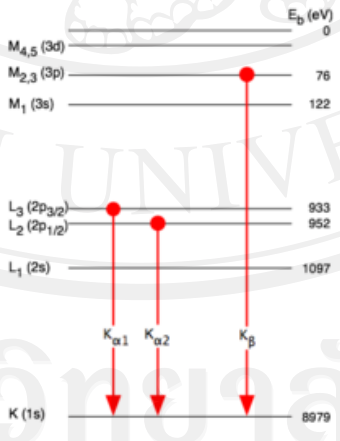

Figure 2.9 Atomic levels involved in copper K_α and K_β emission [19].

For example, the spectrum below is of a high temperature nickel based alloy composed of nickel, chromium, iron, manganese, titanium, molybdenum, silicon, and aluminum detected by the EDS technique Figure 2.10.

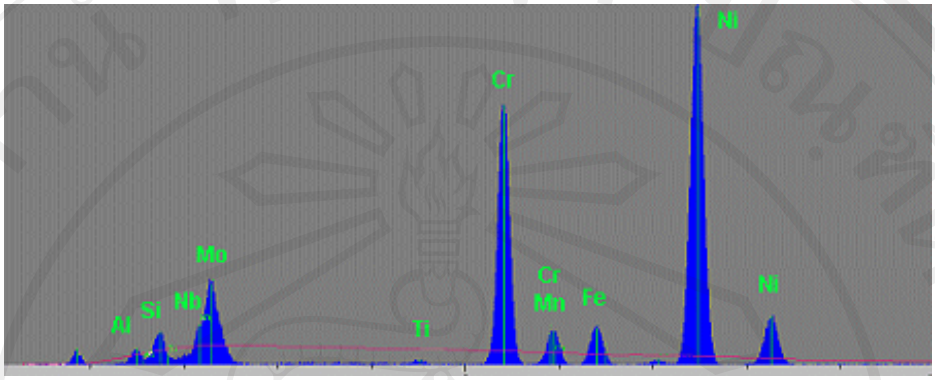

Figure 2.10 The EDS spectrum of a high temperature nickel based alloy which is plotted between the spectrum's energy-count.

The area under each peak in Figure 2.10 can be calculated to provide the percentage of each element composed in the substrate as shown in Table 2.3. One of the most popular calculating algorithms is ZAF where Z stands for the atomic number of the element, A and F are the absorbance and fluorescence values to compensate for the X-ray peak interaction. From this, the atomic and weight percent are calculated [20].

Table 2.3 An example of calculated atomic percentage from Figure 2.10.

Element	Atomic %	Weight %
Al	2.588	1.203
Si	4.247	2.056
Ti	0.365	0.301
Cr	21.793	19.529
Mn	0.229	0.216
Fe	3.931	3.783
Ni	8.337	59.013
Nb	.261	5.221
Mo	.249	8.677

2.6.2 Raman Spectroscopy

Raman spectroscopy is applied to observe vibrational, rotational and other low-frequency modes in a system [21]. The spectroscopy requires a monochromatic light in the visible, near infrared, or near ultraviolet range. The light interacts with substrate molecular vibrations causes excitation mode of molecule. Not only being absorbed and emitted by atoms and molecules, photons may also be scattered, which does not happened because of defects but a molecular effect which provides the way to study energy levels. There are two scattering types happen in the molecule; Elastic scattering and Inelastic scattering.

After a monochromatic laser illuminates sample, the excited molecule emits its energy to reach its ground state by 2 different ways of scattering;

1) If the final vibrational state and the initial vibrational state are the same. It is the elastic scattering or "Rayleigh Scattering".

2) If the final and initial vibrational state are not the same. It is the inelastic scattering. However, the inelastic scattering can be divided into 2 types; Stroke Scattering and Anti-Stroke Scattering

   2.1) If the final vibrational state is more energetic than the initial state. The emitted photon will be shifted to lower frequency in order to balance the total energy of system.

   $n_0 - n_t$

   The shift is called "Strokes shift" and the process is called "Strokes Scattering".

2.2) If the final vibrational state is less energetic than the initial state. The emitted photon will be shifted to higher frequency in order to balance the total energy of system.

$$n_0 + n_t$$

The shift is called "Anti-Stokes shift" and the process is called "Anti-Strokes Scattering" as shown in Figure 2.11.

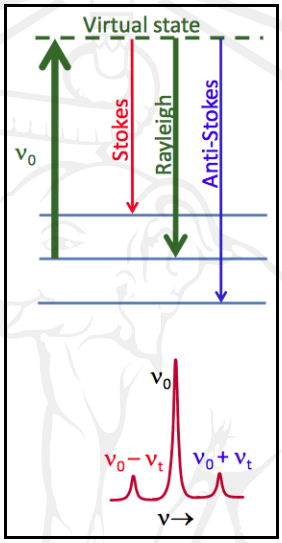

Figure 2.11 The three spectrums and their relative intensity detected after an intense laser beam with frequency n_0 emits onto a material's surface [22].

The elastic Rayleigh scattering is the most intense spectrum; however, it does not contain any characteristic information of the sample, while the Strokes Raman scattering and Anti-Strokes Raman scattering do.

Moreover these scattering processes cause rotation and vibration in molecules. However the vibrational Raman is taking a major role in analyzing the molecules' structure. In additions, there are several theoretical methods to study the vibrational Raman spectrum.

- **Raman spectrum of anatase titanium dioxide [23]**

TiO_2 existed in nature in three different crystal structures; rutile, anatase and brookite. The rutile phase is the common and stable structure of TiO_2; however, the anatase phase in Figure 2.12 is attractive to be studied since the last decade due to its photocatalytic and photovoltaic properties.

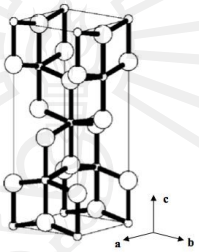

Figure 2.12 Crystal structure of anatase phase. Big and small spheres represent oxygen and titanium atoms, respectively.

Raman intensity of the anatase's wavenumber can be observed at 143 cm^{-1}, 198 cm^{-1}, 396 cm^{-1}, 514 cm^{-1} and 639 cm^{-1}. While the TiO_2 in rutile phase responds to the wavenumber 142, 235, 446 and 609 cm^{-1} as shown in Figure 2.13. The wavenumber 143 cm^{-1} of anatase is very close to the vibrational wavenumber of rutile structure at 142 cm^{-1}, therefore the identification of the peaks intensity between these two wavenumber may not be accurate. As a result, the wavenumber 639 cm^{-1} can determine the amount of anatase phase in film, because it has a relatively higher intensity than the others wavenumber [24].

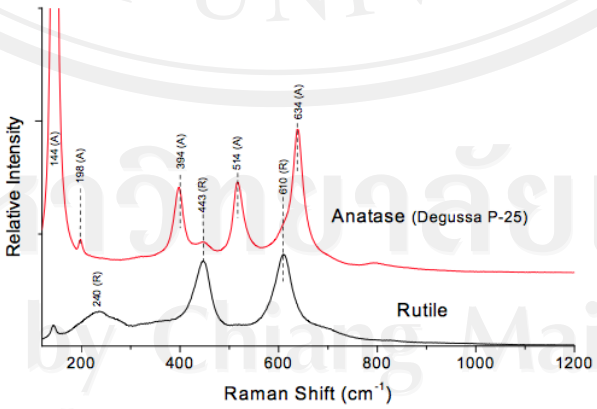

Figure 2.13 The Raman spectrum of (a) anatase TiO_2 (b) rutile TiO_2 [25].

- **Raman spectrum of DLC**

DLC is formed as an amorphous structure which contains a plenty of mixed structure of carbon. Therefore the DLC's spectrum is usually appeared as a several broad peaks. However, the DLC quality is normally defined by the ratio of the amount of sp^3/sp^2 structure which depends on the intensity between the disorder peak (D peak) and the graphite peak (G peak) or I_D/I_G, which respond to the Raman spectrum wavenumbers around 1360 cm^{-1} and 1560 cm^{-1}, which are represented to the breathing mode of sp^2 six-fold rings and sp^2 chains structure respectively as shown in Figure 2.14 and Figure 2.15.

The lower amount of I_D/I_G informs the higher amount of sp^3 structure, which is preferred in the film. Moreover, the more intensity of D peak compared to G peak also causes the shifting of a detected peak of each sample.

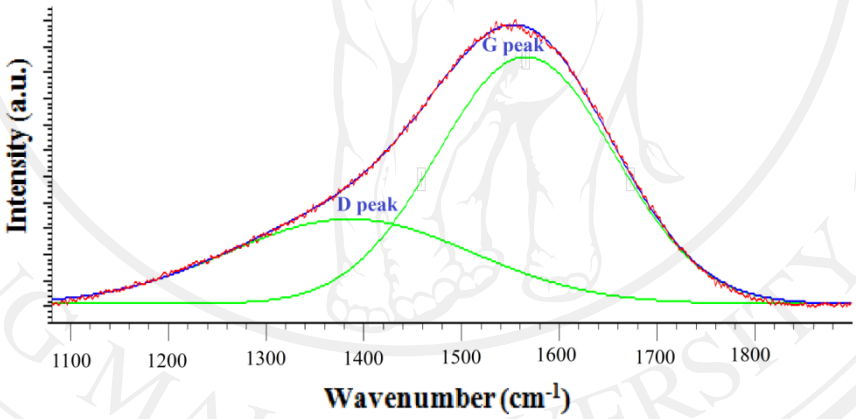

Figure 2.14 Raman spectrum is dominated by G peak (1,560 cm^{-1}) and D peak (1,360 cm^{-1}) of the sp^2 configuration, indirect method on sp^3/sp^2 ratio[7].

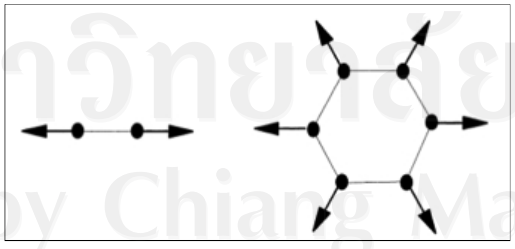

Figure 2.15 The Eigen vectors of Raman sp^2 G and D mode respectively.

2.6.3 Atomic Force Microscopy

Atomic force microscopy is utilized to provide a 3D profile of the film's surface by measuring forces between an AFM probe and the analyzed surface at a very short distance [26]. The force can be described by using Hooke's Law

$$\vec{F} = -k\vec{x}$$

where **F** is the measured force
k is the spring constant
x is the cantilever deflection

If the spring constant of cantilever is less than surface (Normally ~ 0.1-1 N/m), the cantilever bends and the deflection is monitored. As a result, the force is ranging between 10^{-9} to 10^{-6} N.

For the AFM surface analysis, there are several types of forces are measured, the dominant interactions at short probe-sample distances in the AFM are Van der Waals interactions. However long-range interactions are significant further away from the surface. During contact with the sample, the probe predominately experience repulsive Van der Waals forces (contact mode). The leads to the tip deflection described previously. As the tip moves further away from the surface attractive Van der Waals forces are dominant (non-contact mode). Moreover, a fixed wavelength laser is also applied in the AFM to detect the vibration of the tip as shown in Figure 2.16. In additions, there are 3 modes of AFM scanning distinguished by their operation range as shown in Figure 2.17.

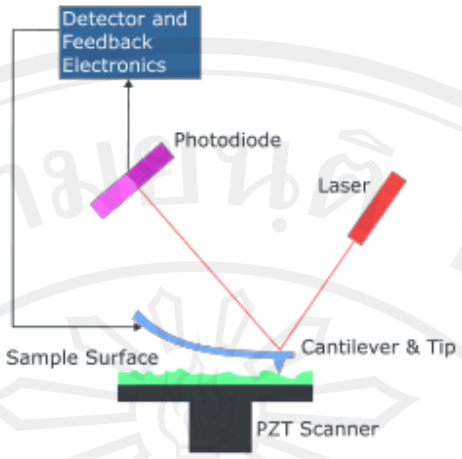

Figure 2.16 A laser beam is in used to provide observing the cantilever movement by the detector.

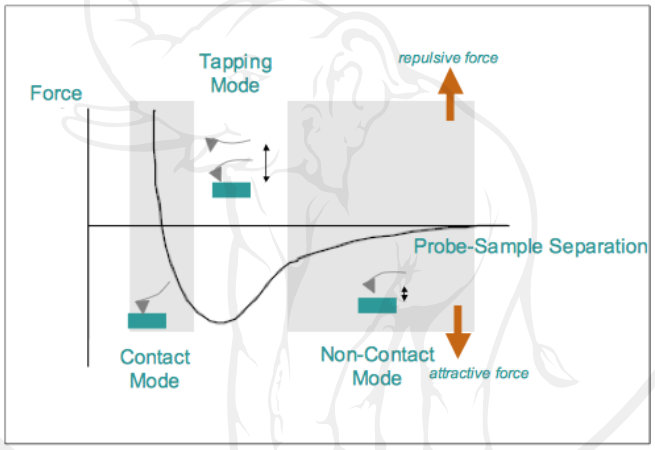

Figure 2.17 Different surface analysis AFM modes identified by their operating range between the AFM's tip and sample's surface.

1) Contact mode

The contact mode considers probe-surface separation is less than 0.5 nm. The tip is forced to be affected by the repulsive force. By maintaining a constant cantilever deflection, the force between the probe and the sample must be constant and an image of the surface is obtained. The advantages of this scanning mode are fast, good for rough samples and used in friction analysis, while its disadvantages is damaging on both cantilever and soft samples.

2) Tapping mode (Intermittent mode)

The tapping mode considers probe-surface separation between 0.5 to 2.0 nm. In this mode, the cantilever is oscillated at its resonant frequency with maintaining constant oscillation amplitude to obtain an image of the surface. The advantages of the tapping mode are providing a high resolution of samples that are easily damaged. While its advantage is slower scanning speed with difficult to analyze surface of liquids materials.

3) Non-contact mode

The non-contact mode considers probe-surface separation between 0.1 to 10 nm. The probe does not contact the sample surface, but oscillates above the scanning surface. Utilizing a feedback loop is required in order to monitor changes in the amplitude due to attractive Van der Waals forces to provide the surface. The advantage of non-contact mode is extending probe lifetime due to very low force exerted on the sample, while its disadvantage is providing generally lower resolution. Therefore, the non-contact mode is the most suitable to apply in this studying.

2.7 Photovoltaic properties efficiency

The efficiency of each photovoltaic cell is defined by its percentage of light-electric power conversion. The easiest way to do the measurement, the photovoltaic cell is installed into an electric circuit as shown in Figure 2.18. After turning on a light source while increasing of the circuit voltage with until the circuit current reach zero, the current-voltage curve is obtained as shown in Figure 2.19.

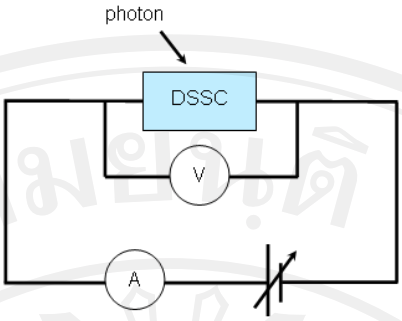

Figure 2.18 Schematic of DSSC photovoltaic properties testing.

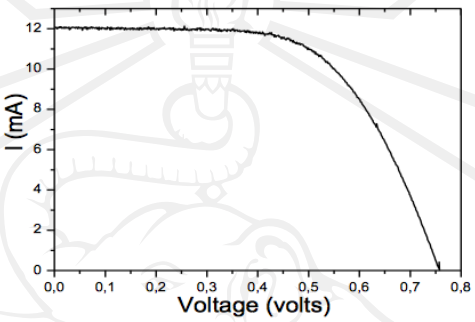

Figure 2.19 An example of the V-I plotted solar cell's photovoltaic properties test.

The well-known power conversion efficiency [27] can be calculated from

$$\eta = \frac{P_m}{P_{in}} \times 100 = \frac{J_{mp} V_{mp}}{P_{in}} \times 100 = \frac{J_{sc} V_{oc} FF}{P_{in}} \times 100$$

where P_m is the maximum power obtained from the cell, P_{in} is the light source's power, J_{sc} is the short circuit current which equals to the maximum current from a solar cell when the voltage across the device is zero, V_{oc} is the open circuit voltage which is the maximum voltage from a solar cell occurs when the net current through the device is zero, J_{mp}, V_{mp}, FF is defined as the ratio of the maximum power from the solar cell to the theoretical obtainable power [28].

$$FF = \frac{\text{maximum obtainable power}}{\text{theoretical obtainable power}} = \frac{J_{mp} V_{mp}}{J_{sc} V_{oc}}$$

In order to calculate the fill factor by the equation above, it is necessary to convert the obtained current-voltage curve into power-voltage curve in Figure 2.20 to obtain J_{mp} and V_{mp}. By with locating the maximum power (P_m) of the power-voltage curve, the V_{mp} and J_{mp} are located at the same point as P_m.

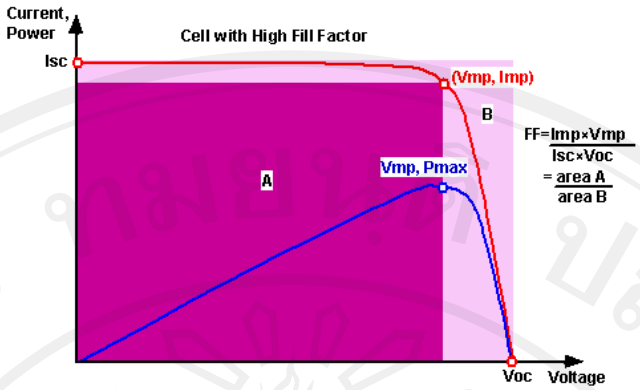

Figure 2.20 (red line) The current-voltage curve obtained from raw data, (blue line) the power-voltage curve obtained from multiplying the current and voltage for each point [28].

Since the input light source power is kept constant at 100 mW and all essential parameters can be obtained from the experiment, the power conversion efficiency can be calculated easily.

2.8 Photocatalytic antibacterial properties

The photocatalytic agent TiO_2, known for its chemical stability and optical competency, has been used extensively for killing different groups of microorganisms including bacteria, fungi and viruses while it is absorbing UV light, because it has high photoreactivity, broad-spectrum antibiosis and chemical stability. Although the TiO_2 with mixed structures is deposited, the anatase is an only phase which has its antibacterial properties [29]. *E. coli* survivability is usually being used to indicate the antibacterial properties.

2.9 Mechanical properties of DLC

DLC film is required to be characterized its hardness and adhesion. The hardness of the film is defined as

$$H = \frac{F_{max}}{A}$$

Where F_{max} is the maximum load which causes a constant penetration depth.

A is the projected contact area.

The variables are measured by using Hysitron™ triboindenter as shown in Figure 2.21.

Figure 2.21 Hysitron™ triboindenter plays a role measure the films' hardness and adhesion.

The hardness of the film is not only one necessary properties but the adhesion is also important. In order to measure the film's adhesion, the film's surface is being applied by normal force which initially set at a low level and continues increase while the substrate is dragging in the horizontal direction as shown in Figure 2.22. The friction force is measured during the applying force to detect the adhesive failure at a point called "Critical load" where the friction force is abrupt increased. Moreover, the measured critical load can be implied to the adhesion of the film as shown in Figure 2.23.

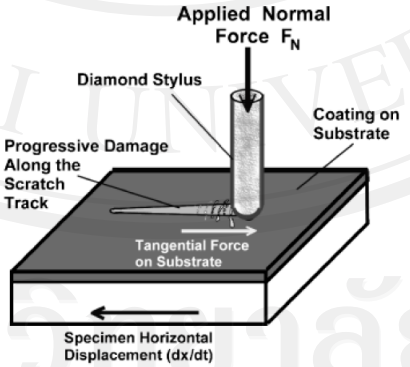

Figure 2.22 The specimen is dragging in the horizontal direction while the applied normal force is increasing overtime.

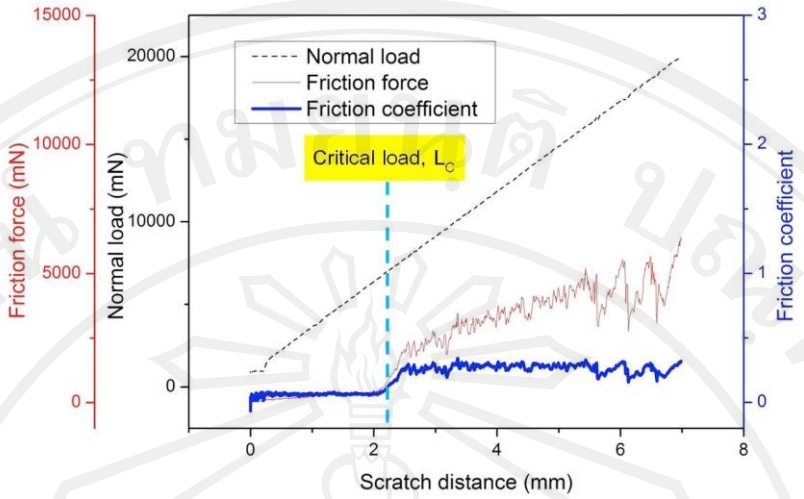

Figure 2.23 The increasing applied normal force is measured overtime to detect the critical load where the friction force increases suddenly.